Landes Bioscience

www.landesbioscience.com

Supplemental Material to:

Maria Bouvy-Liivrand, Merja Heinäniemi, Elisabeth John, Jochen G Schneider, Thomas Sauter, Lasse Sinkkonen

Combinatorial regulation of lipoprotein lipase by microRNAs during mouse adipogenesis

2013; 11(1)

http://dx.doi.org/10.4161/rna.27655

www.landesbioscience.com/journals/rnabiology/article/27655/

SUPPLEMENTARY MATERIAL

SUPPLEMENTARY TEXT

Mathematical model (Systems Biology Toolbox 2 format)

********** MODEL NAME

Combinatorial regulation of lipoprotein lipase by microRNAs during mouse adipogenesis

********** MODEL NOTES

Systems Biology Toolbox 2 model by:

Thomas Sauter, Maria Liivrand, Lasse Sinkkonen

University of Luxembourg, January 2013

Email: thomas.sauter@uni.lu

Parameter set: Best fit of time course 2

Initial conditions: Steady state values for these parameters with Xc=Rosi=0 and Xm27=Xm29=1

********** MODEL STATES

d/dt(Cebpa) = r_1 + r_3 + r_10 - r_15

d/dt(CEBPA) = r_7 - r_16

d/dt(Lpl27) = ratio*r_14 - r_17

d/dt(Lpl29) = ratio*r_13 - r_18

d/dt(Lpl) = r_2 + r_11 - r_13 - r_14 - r_21

d/dt(MIR27a) = r_5 - ratio*r_12 - ratio*r_14 - r_19

d/dt(MIR29a) = r_6 - ratio*r_13 - r_20

d/dt(Pparg27) = ratio*r_12 - r_24

d/dt(Pparg) = r_4 + r_8 - r_12 - r_22

d/dt(PPAR) = r_9 - r_23

Cebpa(0) = 0.0145

CEBPA(0) = 0.0034

Lpl27(0) = 0

Lpl29(0) = 0

Lpl(0) = 0.0657

MIR27a(0) = 0.543

MIR29a(0) = 1

Pparg27(0) = 0

Pparg(0) = 0.0216

PPAR(0) = 0.0108

********** MODEL PARAMETERS

ac = 0.00032746

al = 0.089728

acbasal = 0.17165

apbasal = 0.059056

ratioPPAR27 = 0.5434

cLPL27 = 0.0035711

ratioLPL29 = 0.84611

eCEBPA = 3.8376

eCEBPAP = 8.0636

ePPAR = 4.9943

eCPPARP = 40.529

eLPPARP = 21.702

dCEBPA = 11.94

dPPAR = 3.9995

dCEBPAP = 16.248

dM27 = 0.38249

dM29 = 0.16052

dLPL = 1.37

dPPARP = 9.9901

kPPARligint= 0.0024599

Xm27_D0 = 0.50092

ratio= 0.009562

Xc = 0

Xm27 = 1

Xm29 = 1

Rosi = 0

ratio2729=0.543

********** MODEL VARIABLES

meas27 = MIR27a + Lpl27 + Pparg27

meas29 = MIR29a + Lpl29

********** MODEL REACTIONS

r_1=ac*Xc

r_2=al

r_3=acbasal

r_4=apbasal

r_5=dM27*Xm27*ratio2729

r_6=dM29*Xm29

r_7=eCEBPA*Cebpa

r_8=eCEBPAP*CEBPA

r_9=ePPAR*Pparg

r_10=eCPPARP*PPAR*(kPPARligint+Rosi)

r_11=eLPPARP*PPAR*(kPPARligint+Rosi)

r_12=ratioPPAR27*cLPL27*MIR27a*Pparg

r_13=ratioLPL29*cLPL27*MIR29a*Lpl

r_14=cLPL27*MIR27a*Lpl

r_15=dCEBPA*Cebpa

r_16=dCEBPAP*CEBPA

r_17=dM27*Lpl27

r_18=dM29*Lpl29

r_19=dM27*MIR27a

r_20=dM29*MIR29a

r_21=dLPL*Lpl

r_22=dPPAR*Pparg

r_23=dPPARP*PPAR

r_24=dM27*Pparg27

********** MODEL FUNCTIONS

********** MODEL EVENTS

********** MODEL MATLAB FUNCTIONS

SUPPLEMENTARY TABLES

Table S1: siRNA sequences. The sequences of siRNAs used in this study are provided.

siRNA	**Sequence (5' – 3')**
si*Pparg-1*	CCAUCCGAUUGAAGCUUAU
si*Pparg-2*	CAACAGGCCUCAUGAAGAA
si*Pparg-3*	GUUGAUUUCUCCAGCAUUU
si*Control*	UGCGCUACGAUCGACGAUG

Table S2: Primer pairs for RT-qPCR. The sequences of primer pairs used are provided.

Primer pair	**Sequence (5' - 3')**
Cebpa	GAGCTGAGTGAGGCTCTCATTCT TGGGAGGCAGACGAAAAAAC
Lpl	GACTCTGTGTCTAACTGCCACTTCA CCCGTTACCGTCCATCCAT
Pparg	CACAAGAGCTGACCCAATGGT GATCGCACTTTGGTATTCTTGGA
Rpl13a	TGGTCCCTGCTGCTCTCA CCCCAGGTAAGCAAACTTTCT

Table S3: Details on parameters of the mathematical model. Parameter names, the corresponding reactions and a short description are given in columns A-C. Lower and upper bounds (columns D-E) were applied during the parameter estimation (see Materials and Methods). The model was fitted to the three differentiation time courses separately. Mean and relative standard deviation of the selected good fits per differentiation are given in columns G-N. The parameter values of the best obtained fit per differentiation are given in columns P-R. The simulation and prediction figures were obtained by simulating all obtained good parameter sets and taking the median +/- 68% range (see Material and Methods)

Parameter					**Differentiation 1**		**Differentiation 2**		**Differentiation 3**		**Best fits:**		
unit: [1/d]	in reaction:	description:	lower bound	upper bound	Mean	rel Std	Mean	real Std	Mean	rel Std	Time course1	Time course 2	Time course 3
ac	r_1	input (Xc)-dependent transcription of Cebpa	0	1000	0.0748	1.9933	0.0026	2.9421	0.004	3.0207	0.23951	0.00032746	0.0021402
al	r_2	basal transcription of Lpl	0	1000	0.9182	0.9378	0.147	1.3805	0.2326	2.2173	0.86591	0.089728	0.064742
acbasal	r_3	basal transcription of Cebpa	0	1000	0.3057	0.8217	0.1362	1.0578	0.1103	1.2617	0.34772	0.17165	0.095665
apbasal	r_4	basal transcription of Pparg	0	1000	0.161	0.5913	0.0787	0.7116	0.0835	0.6299	0.17548	0.059056	0.073514
ratioPPAR27	r_12	ratio of miR27a Pparg complex formation to miR27a Lpl complex formation	0.5	2	1.5551	0.3123	1.2493	0.4276	1.2758	0.4592	1.9986	0.5434	1.4212
cLPL27	r_14, (r_12, r_13)	miR27a Lpl complex formation	0	10	2.7275	0.9121	1.5912	1.527	1.462	1.7212	2.4017	0.0035711	0.001273
ratioLPL29	r_13	ratio of miR29a Lpl complex formation to miR27a Lpl complex formation	0.5	2	0.6808	0.5564	0.8526	0.5616	1.0139	0.5218	0.51242	0.84611	0.50309
eCEBPA	r_7	translation of CEBPA	0	1000	197.6492	1.6836	163.5129	1.857	154.2769	2.0026	81.606	3.8376	24.138
eCEBPAP	r_8	CEBPA-dependent transcription of Pparg	0	1000	28.6422	4.1834	35.2276	4.1192	41.3223	3.9706	0.3885	8.0636	1.0396
ePPAR	r_9	translation of PPARG	0	1000	123.9134	1.9842	72.898	2.6335	128.895	1.9603	383.15	4.9943	39.388
eCPPARP	r_10	partially input (Rosi)-dependent PPARG-dependent transcription of Cebpa	0	1000	114.1534	1.8361	92.6377	2.0574	137.9765	1.8825	0.60585	40.529	6.1873
eLPPARP	r_11	partially input (Rosi)-dependent PPARG-dependent transcription of Lpl	0	1000	98.865	1.9117	79.1107	2.004	93.96	1.8784	0.45469	21.702	3.2646
dCEBPA	r_15	degradation of Cebpa	9	12	11.3062	0.0865	10.9618	0.1035	10.9933	0.1071	11.985	11.94	11.959
dPPAR	r_22	degradation of Pparg	3	4	3.8021	0.0886	3.8447	0.0743	3.8149	0.0842	3.9938	3.9995	3.9996
dCEBPAP	r_16	degradation of CEBPA	9	17	14.1345	0.2116	13.8116	0.2182	14.3909	0.2062	16.964	16.248	16.862
dM27	r_5, r_17, r_19, r_24	degradation and input (Xm27)-dependent transcription of miR27a	0.11	0.4	0.4006	0.1449	0.3486	0.2975	0.2511	0.4923	0.42	0.38249	0.15686
dM29	r_6, r_18, r_20	degradation and input (Xm29)-dependent transcription of miR29a	0.11	0.4	0.1109	0.0177	0.157	0.0541	0.25	0.2004	0.11037	0.16052	0.23098
dLPL	r_21	degradation of Lpl	0.83	1.66	1.5581	0.1244	1.3439	0.1771	1.5469	0.1496	1.641	1.37	1.6586
dPPARP	r_23	degradation of PPARG	3	10	8.6729	0.2194	8.083	0.2633	8.1331	0.2718	9.9867	9.9901	9.8421
kPPARligint	r_10, r_11	relative internal ligand concentration activating PPARG	0	0.5	0.0851	1.6058	0.0491	1.9462	0.0355	2.7559	0.0012564	0.0024599	0.00065546
Xm27_D0	r_5	miR27a transcription activating input level from D0 on	0	1	0.6684	0.1769	0.4563	0.3989	0.1637	1.2332	0.70824	0.50092	0.0014839
ratio	r_12, r_13, r_14	ratio of mRNA to miRNA molecules	0.001	0.01	0.0023	1.042	0.0028	0.9296	0.0035	0.8845	0.0016473	0.009562	0.0041764
Fixed experiment specific:													
ratio2729	r_5	experiment specific ratio of miR27a to miR29a	---	---	---	---	---	---	---	---	0.509	0.543	0.5308

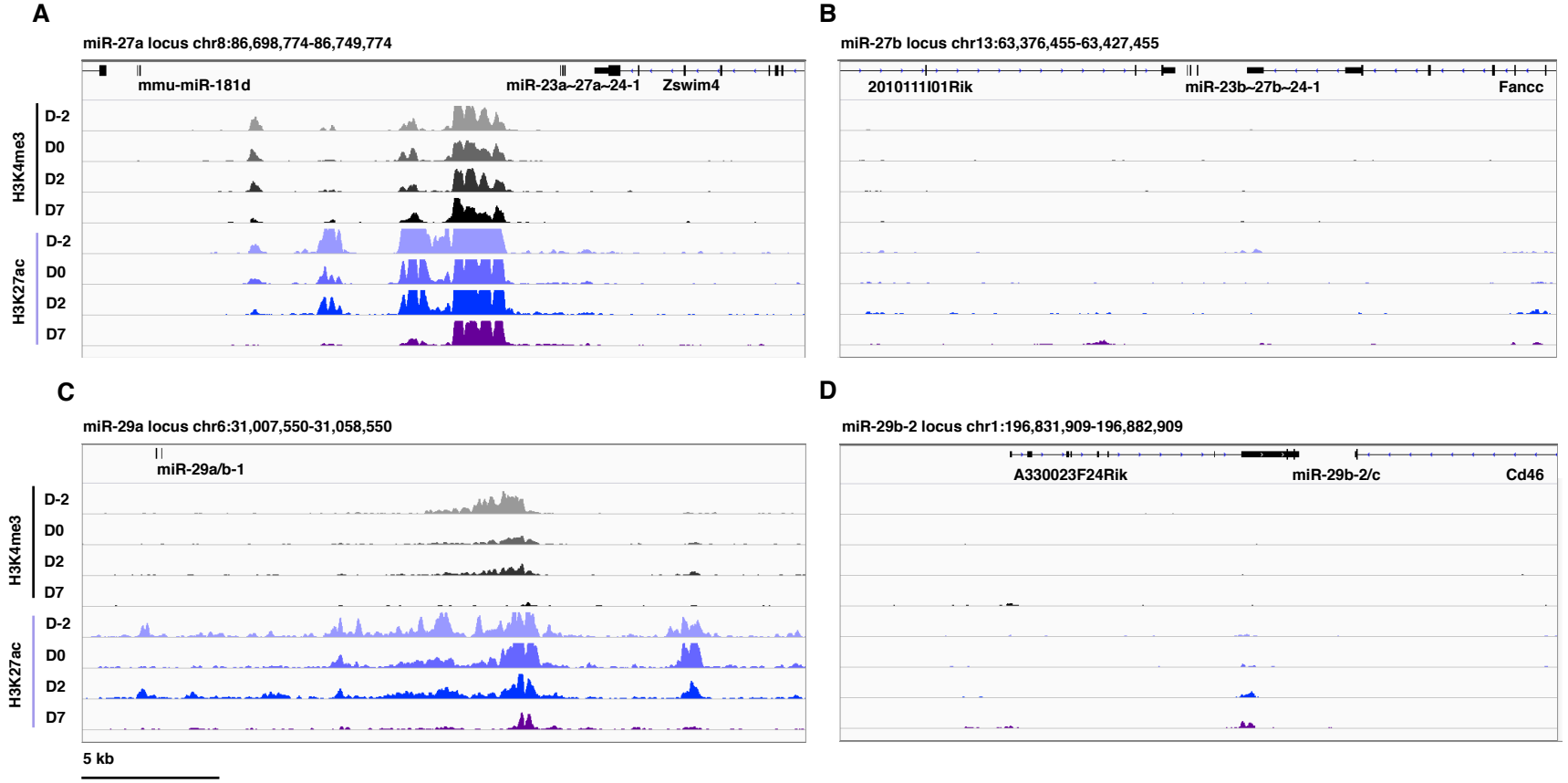

Supplementary Figure S1. Changes in the levels of histone modifications H3K4me3 and H3K27ac in the vicinity of miR-27 and miR-29 family clusters. Enrichment of histone H3K4 trimethylation and H3K27 acetylation have been shown to correlate closely with proximal and/or distal active promoter regions, respectively. Presented dataset (GEO GSE20752) shows the dynamic development of modification patterns over 7 days of 3T3-L1 cell line differentiation for (A) miR-27a (miR-23a~27a~24-2 cluster), (B) miR-27b (miR-23b~27b~24-1 cluster), (C) miR-29a (miR-29a/b-1 cluster) and (D) miR-29b (miR-29c/b-2 cluster). Track height is set identically to 100 on all panels. Modified from Integrated Genomics Viewer.

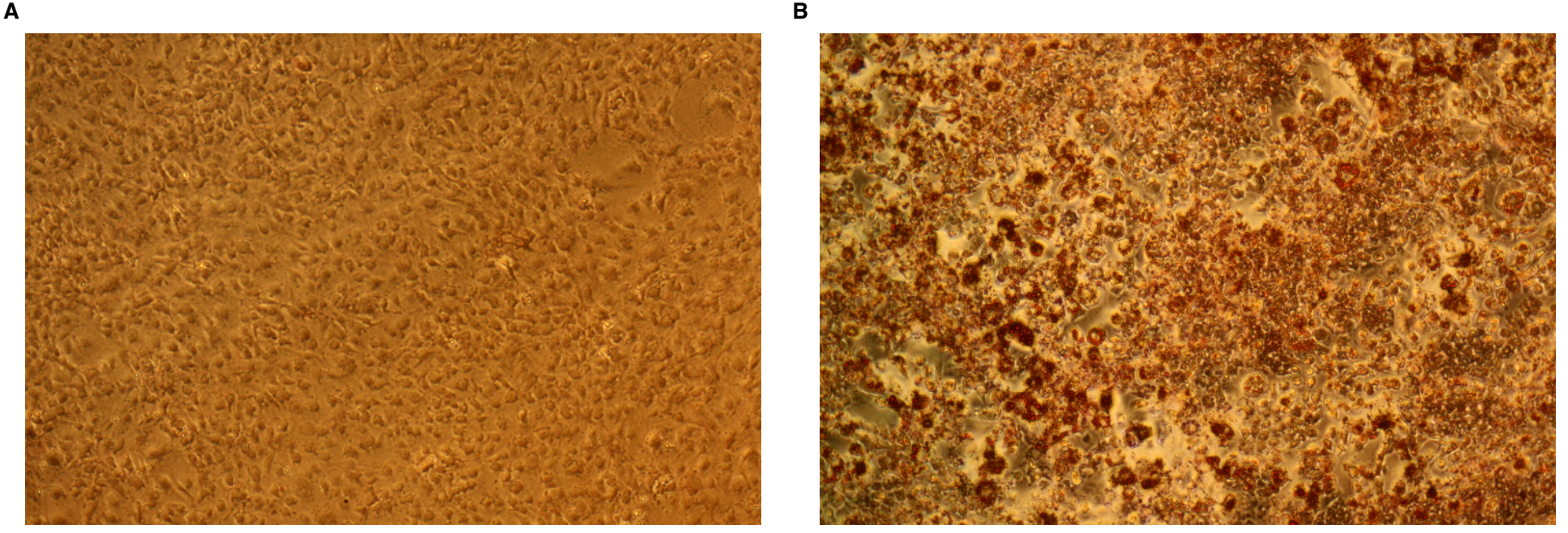

Supplementary Figure S2. Oil Red O staining of lipids in D0 (A) and D8 (B) differentiated 3T3-L1 cells was used to control the differentiation of the adipocytes. Representative images after Oil Red O stainings showing that D0 cells contain no or very little lipids while D8 cells have high accumulation of lipids in most cells, indicating efficient differentiation. Presented images correspond to the experiments in Supplementary Figure S5.

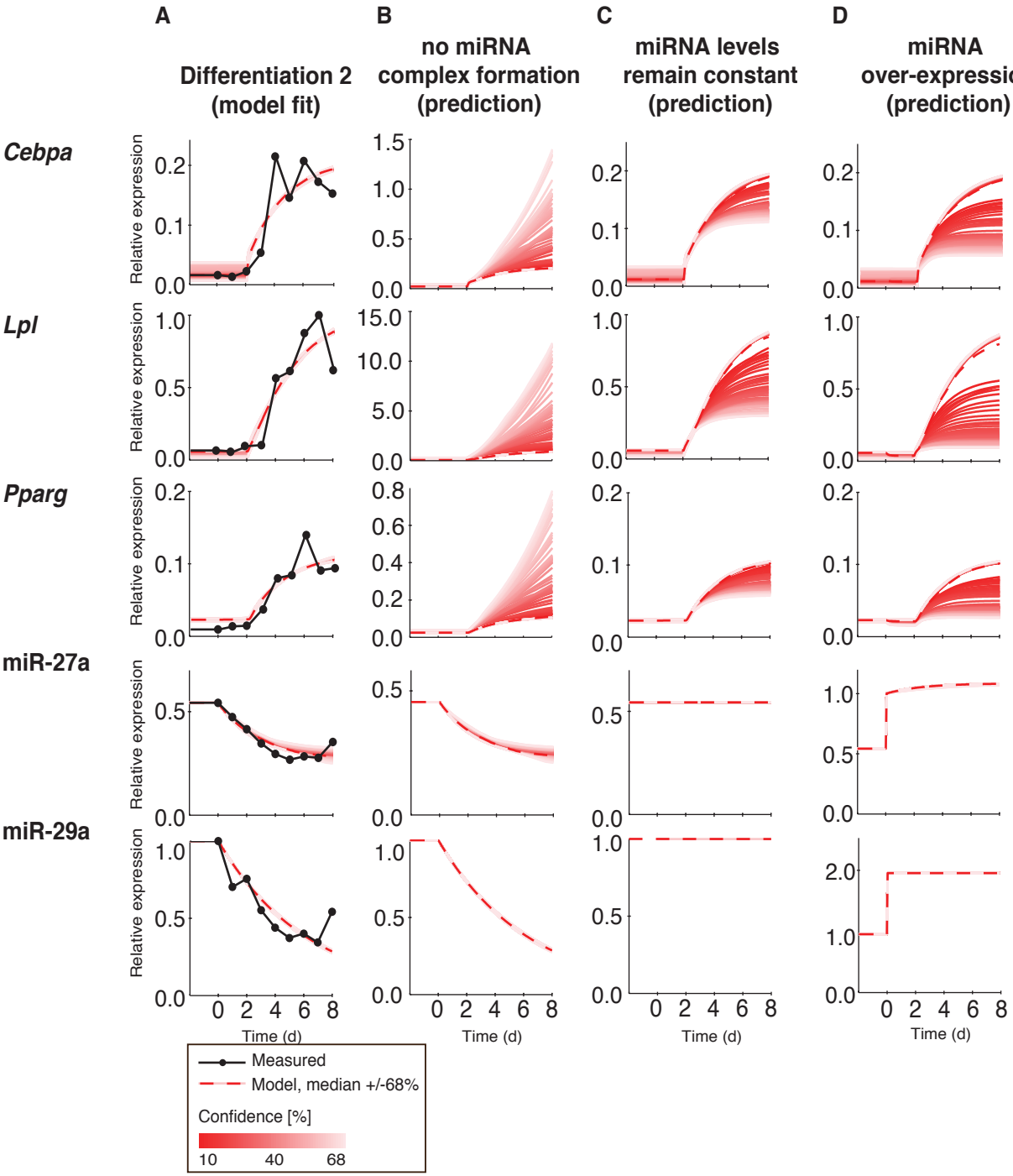

Supplementary Figure S3. In silico model predictions for target mRNA level changes in response to miRNA perturbations during Differentiation 2. The fitted model (A) predicts for the target mRNAs, especially Lpl, a stronger and faster upregulation when miRNA-target complexes are not forming (B); weaker and delayed mRNA upregulation when miRNA levels remain at Day 0 levels (C); up to 80% reduction in Lpl upregulation when the miRNAs are two-fold over-expressed at differentiation start (D). Black dotted line represents measured mRNA levels and the red dashed line represents the median of all iterations of the model fit within an optimal cost threshold of 1.33-fold of the best obtained fit, respectively the median of the predictions obtained by using these selected model fits, with red fading up to +/-68% of confidence levels. Measured mRNA expression values are normalized to highest mRNA data point and measured miRNA expression values are normalized to highest miRNA data point. All axes and data points correspond directly to measured cDNA ratios. Confidence intervals are 68% for shown fits.

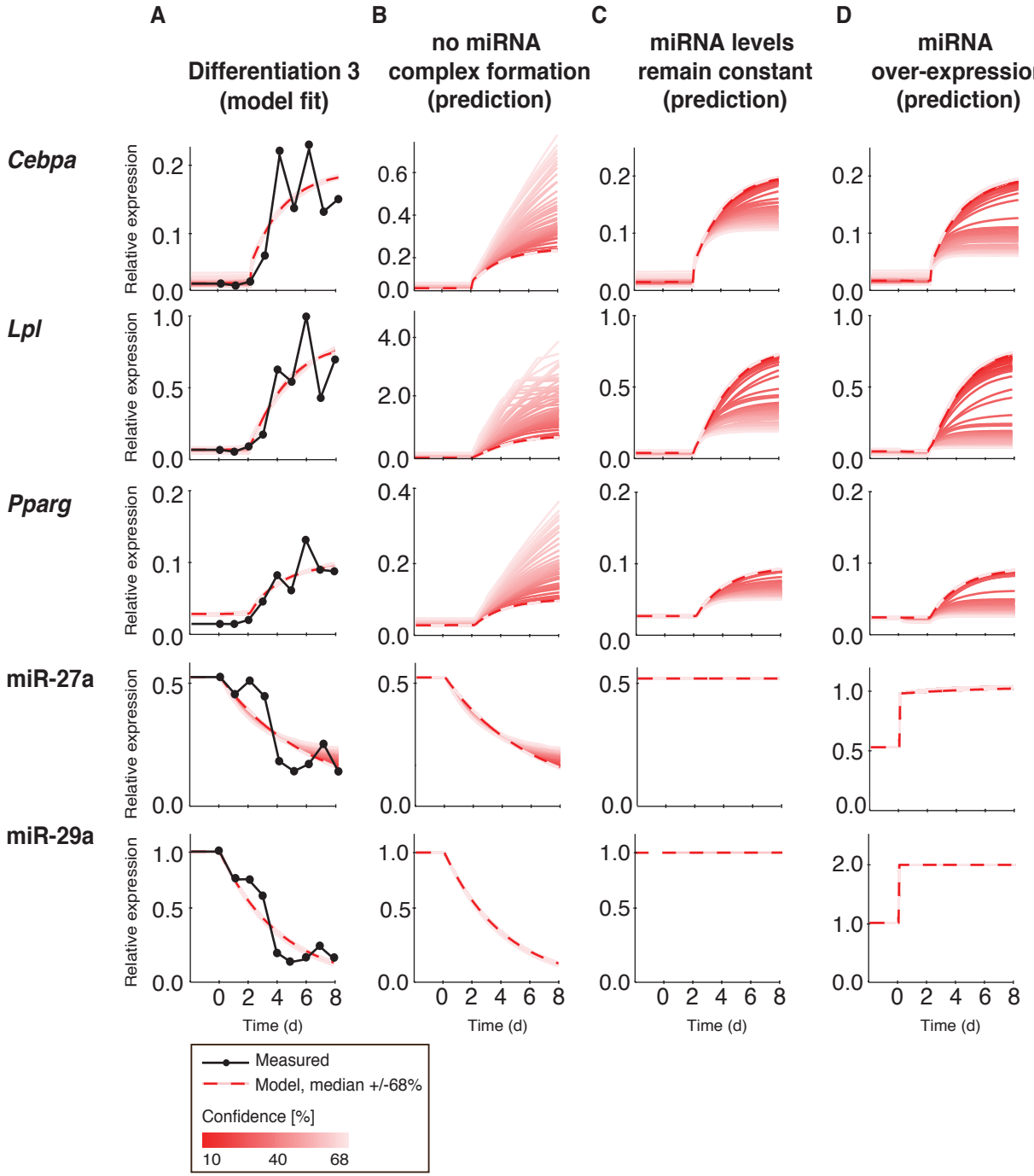

Supplementary Figure S4. In silico model predictions for target mRNA level changes in response to miRNA perturbations during Differentiation 3. See figure legend S3 for more details.

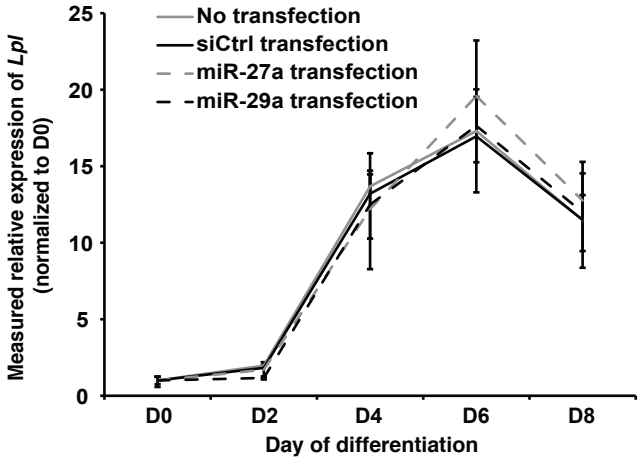

Supplementary Figure S5. Impact of transient overexpression of individual miRNAs in pre-adipocytes on *Lpl* expression during 3T3-L1 adipocyte differentiation. The level of *Lpl* mRNA was quantified with gene specific primers during induced adipogenesis of 8 days in the mouse 3T3-L1 cell line following either a transient transfection of 25 nM siControl, miR-27a mimic, miR-29a mimic or no transfection. Measured expression values were normalized to *Rpl13a* mRNA and presented as relative to D0 that is set to 1. The data indicate the mean expression values of three independent experiments and the error bars represent SEM.